Theory of negative refraction in periodic stratified metamaterials

Ivan D. Rukhlenko,[1] **Malin Premaratne,**[1] **and Govind P. Agrawal**[2]

[1]*Advanced Computing and Simulation Laboratory (AχL), Department of Electrical and Computer Systems Engineering, Monash University, Clayton, VIC 3800, Australia*
[2]*Institute of Optics, University of Rochester, Rochester, New York 14627, USA*
ivan.rukhlenko@monash.edu

Abstract: We present a general theory of negative refraction in periodic stratified heterostructures with an arbitrary number of homogeneous, isotropic, nonmagnetic layers in a unit cell. With a 4×4-matrix technique, we derive analytic expressions for the normal modes of such a heterostructure slab, introduce the average refraction angles of the energy flow and wavevector for the TE- and TM-polarized plane waves falling obliquely on the slab, and derive expressions for the reflectivity and transmissivity of the whole slab. For a specific case, in which all layers in a unit cell are much thinner than the wavelength of light, we obtain approximate simple formulae for the effective refraction angles. Using the example of a semiconductor heterostructure slab with two layers in a unit cell, we demonstrate that ultrathin layers are preferable for metamaterial applications because they enable higher transmissivity within the frequency band of negative refraction. Our theory can be used to study the optical properties of any stratified metamaterial, irrespective of whether semiconductors or metals are employed for fabricating its various layers, because it includes absorption within each layer.

OCIS codes: (160.3918) Metamaterials; (260.2110) Electromagnetic optics; (310.6860) Thin films, optical properties; (999.9999) Negative refraction.

References and links

1. V. M. Shalaev, "Optical negative index metamaterials," Nature Photon. **1**, 41–47 (2007).
2. V. A. Podolskiy and E. E. Narimanov, "Strongly anisotropic waveguide as a nonmagnetic left-handed system," Phys. Rev. B **71**, 201101 (2005).
3. J. B. Pendry, "A chiral route to negative refraction," Science **306**, 1353–1355 (2004).
4. N. C. Panoiu and R. M. Osgood, "Numerical investigation of negative refractive index metamaterials at infrared and optical frequencies," Opt. Commun. **233**, 331–337 (2003).
5. R. A. Shelby, D. R. Smith, and S. Schultz, "Experimental verification of a negative index of refraction," Science **292**, 77–79 (2001).
6. D. R. Smith, W. J. Padilla, D. C. Vier, S. C. Nemat-Nasser, and S. Schultz, "Composite medium with simultaneously negative permeability and permittivity," Phys. Rev. Lett. **84**, 4184–4187 (2000).
7. A. Boltasseva and V. M. Shalaev, "Fabrication of optical negative-index metamaterials: recent advances and outlook," Metamaterials **2**, 1–17 (2008).
8. W. Cai, U. K. Chettiar, A. V. Kildishev, and V. M. Shalaev, "Optical cloaking with metamaterials," Nature Photon. **1**, 224–227 (2007).
9. J. B. Pendry, D. Schurig, and D. R. Smith, "Controlling electromagnetic fields," Science **312**, 1780–1782 (2006).
10. T. J. Yen, W. J. Padilla, N. Fang, D. C. Vier, D. R. Smith, J. B. Pendry, D. N. Basov, and X. Zhang, "Terahertz magnetic response from artificial materials," Science **303**, 1494–1496 (2004).
11. S. Linden, C. Enkrich, M. Wegener, J. Zhou, T. Koschny, and C. M. Soukoulis, "Magnetic response of metamaterials at 100 terahertz," Science **306**, 1351–1353 (2004).

#138472 - $15.00 USD Received 19 Nov 2010; revised 15 Dec 2010; accepted 15 Dec 2010; published 17 Dec 2010

12. G. Dolling, M. Wegener, C. M. Soukoulis, and S. Linden, "Negative-index metamaterial at 780 nm wavelength," Opt. Lett. **32**, 53–55 (2007).
13. G. Dolling, C. Enkrich, M. Wegener, C. M. Soukoulis, and S. Linden, "Low-loss negative-index metamaterial at telecommunication wavelengths," Opt. Lett. **31**, 1800–1802 (2006).
14. S. Zhang, W. Fan, K. J. Malloy, S. R. J. Brueck, N. C. Panoiu, and R. M. Osgood, "Demonstration of metal-dielectric negative-index metamaterials with improved performance at optical frequencies," J. Opt. Soc. Am. B **23**, 434–438 (2006).
15. V. G. Veselago, L. Braginsky, V. Shklover, and Ch. Hafner, "Negative refractive index materials," J. Comput. Theor. Nanosci. **3**, 189–218 (2006).
16. V. M. Shalaev, W. Cai, U. K. Chettiar, H. K. Yuan, A. K. Sarychev, V. P. Drachev, and A. V. Kildishev, "Negative index of refraction in optical metamaterials," Opt. Lett. **30**, 3356–3358 (2006).
17. T. A. Klar, A. V. Kildishev, V. P. Drachev, and V. M. Shalaev, "Negative-index metamaterials: Going optical," IEEE J. Sel. Top. Quant. Electron. **12**, 1106–1115 (2006).
18. C. Enkrich, M. Wegener, S. Linden, S. Burger, L. Zschiedrich, F. Schmidt, J. F. Zhou, T. Koschny, and C. M. Soukoulis, "Magnetic metamaterials at telecommunication and visible frequencies," Phys. Rev. Lett. **95**, 203901 (2005).
19. A. J. Hoffman, L. Alekseyev, S. S. Howard, K. J. Franz, D. Wasserman, V. A. Podolskiy, E. E. Narimanov, D. L. Sivco, and C. Gmachl, "Negative refraction in semiconductor metamaterials," Nature Mater. **6**, 946–950 (2007).
20. A. V. Kildishev and E. E. Narimanov, "Impedance-matched hyperlens," Opt. Lett. **32**, 3432–3434 (2007).
21. E. E. Narimanov and V. M. Shalaev, "Optics: Beyond diffraction," Nature **447**, 266–267 (2007).
22. W. Cai, D. A. Genov, and V. M. Shalaev, "Superlens based on metal-dielectric composites," Phys. Rev. B **72**, 193101 (2005).
23. J. B. Pendry, "Negative refraction makes a perfect lense," Phys. Rev. Lett. **85**, 3966–3969 (2000).
24. V. G. Veselago, "The electrodynamics of substances with simultaneously negative values of ε and μ," Sov. Phys. Usp. **10**, 509–514 (1968).
25. U. K. Chettiar, A. V. Kildishev, H. K. Yuan, W. Cai, S. Xiao, V. P. Drachev, and V. M. Shalaev, "Dual-band negative index metamaterial: Double negative at 813 nm and single negative at 772 nm," Opt. Lett. **32**, 1671–1673 (2007).
26. S. Zhang, W. Fan, K. J. Malloy, S. R. J. Brueck, N. C. Panoiu, and R. M. Osgood, "Near-infrared double negative metamaterials," Opt. Express **13**, 4922–4930 (2005).
27. H. O. Moser, B. D. F. Casse, O. Wilhelmi, and B. T. Saw, "Terahertz response of a microfabricated rodsplit-ring-resonator electromagnetic metamaterial," Phys. Rev. Lett. **94**, 063901 (2005).
28. T. Koschny, M. Kafesaki, E. N. Economou, and C. M. Soukoulis, "Effective medium theory of left-handed materials," Phys. Rev. Lett. **93**, 107402 (2004).
29. V. P. Drachev, U. K. Chettiar, A. V. Kildishev, H. K. Yuan, W. Cai, and V. M. Shalaev, "The Ag dielectric function in plasmonic metamaterials," Opt. Express **16**, 1186–1195 (2008).
30. H. K. Yuan, U. K. Chettiar, W. Cai, A. V. Kildishev, A. Boltasseva, V. P. Drachev, and V. M. Shalaev, "A negative permeability material at red light," Opt. Express **15**, 1076–1083 (2007).
31. S. Zhang, W. Fan, B. K. Minhas, A. Frauenglass, K. J. Malloy, and S. R. J. Brueck, "Midinfrared resonant magnetic nanostructures exhibiting a negative permeability," Phys. Rev. Lett. **94**, 037402 (2005).
32. M. Born and E. Wolf, *Principles of Optics* (Cambridge U. Press, 1999).
33. P. Yeh, A. Yariv, and C.-S. Hong, "Electromagnetic propagation in periodic stratified media. I. General theory," J. Opt. Soc. Am. **67**, 423–438 (1976).
34. D. W. Berreman, "Optics in stratified and anisotropic media: 4×4-matrix formulation," J. Opt. Soc. Am. **62**, 502–510 (1972).
35. V. M. Shalaev, *Nonlinear Optics of Random Media: Fractal Composites and Metal-Dielectric Films* (Springer, Berlin, 2000).
36. D. W. Berreman and T. J. Scheffer, "Order versus temperature in cholesteric liquid crystals from reflectance spectra," Phys. Rev. A **5**, 1397–1403 (1972).
37. D. W. Berreman and T. J. Scheffer, "Bragg reflection of light from single-domain cholesteric liquid-crystal films," Phys. Rev. Lett. **25**, 577–581 (1970).

1. Introduction

Within the last several years, interest in man-made composites, known as metamaterials, has grown rapidly due to their potential to revolutionize optical technologies [1–6]. Owing to an artificially engineered subwavelength structure, metamaterials exhibit novel electromagnetic properties that are far beyond those available with ordinary materials existing in nature. In particular, the design of meta-atoms allows strong interaction of the magnetic field of an electromagnetic wave with the metamaterial, leading to a variety of beneficial applications [7–11].

#138472 - $15.00 USD Received 19 Nov 2010; revised 15 Dec 2010; accepted 15 Dec 2010; published 17 Dec 2010

Several promising applications are associated with the phenomenon of negative refraction, occurring when an incoming optical wave bends in such a manner that the incident and refraction angles have opposite signs. More importantly, recent advances in modern nanotechnology enable fabrication of metal-dielectric composites that possess a negative refractive index at optical frequencies [12–19]. Such metamaterials have led to the concept of "perfect" lens that can be used for imaging objects with a subwavelength resolution [19–23].

In general, a metamaterial exhibits negative refraction in a spectral range over which real parts of both the permittivity and permeability are negative [6,24]. This situation can be realized by creating metamaterials with overlapping resonances for the functions $\varepsilon(\omega)$ and $\mu(\omega)$ [5,25–28]. Recently, a simpler way to attain a negative refractive index has been proposed [2]. Instead of simultaneously producing electric and magnetic resonances in one metamaterial, one can fabricate a periodic stratified heterostructure using alternating layers of two ordinary materials, only one of which has $\mathrm{Re}\,\varepsilon < 0$ (or $\mathrm{Re}\,\mu < 0$) within a certain frequency band. Because of the anisotropic nature of such a heterostructure, it exhibits the phenomenon of negative refraction with respect to either a TM- or TE-polarized beam, depending on whether its permittivity or permeability has a resonance [19, 29–31].

To harness the full potential of such stratified periodic metamaterials, a comprehensive theory capable of explaining their behavior is required. Although ample theoretical efforts have been made to study optical response of thin films and periodic layered heterostructures [32–34], these results cannot be directly used to analyze negative-index metamaterials. In this paper, we fill this gap by developing a comprehensive theory of stratified nonmagnetic metamaterials exhibiting negative refraction. Following Berreman [34], we discuss in Section 2 the general solution of Maxwell's equations for a layered heterostructure in the 4×4 matrix representation. Using this solution, we find the eigenvalues of the translation matrix, and the corresponding normal modes, for a multilayer slab. The normal modes are then used to define the average refraction angles for energy flow and wavevector as well as to calculate the transmissivity and reflectivity of a multilayer slab. In many practical situations, the layers of stratified metamaterial are much thinner then the wavelength of light, and the effective medium approximation is valid [22,28,35]. This regime is considered in Section 3. We illustrate our general theory in Section 4 through an example of an all-semiconductor heterostructure, used originally to demonstrate the phenomenon of negative refraction in the long-wavelength infrared region.

2. Light propagation through a slab of periodic stratified heterostructure

To describe the phenomenon of negative refraction, we use an elegant 4×4-matrix technique, developed initially to study the optical properties of liquid-crystal films [36, 37]. We briefly discuss the idea behind this technique, before employing it to calculate the refraction angles for energy flux and wavefront, as well as the transmission and reflection coefficients for a plane wave falling obliquely on a periodic stratified heterostructure.

2.1. 4×4*-matrix formalism*

Consider a plane electromagnetic wave of frequency ω, incident at an angle ϑ_0 on the surface $z = 0$ of a stratified periodic heterostructure slab, as shown in Fig. 1. Each unit cell of this slab contains n layers of different thicknesses h_j and different permittivities $\varepsilon_j(\omega)$ ($j = 1,2,\ldots,n$). Each layer is composed of a homogeneous, isotropic material so that ε_j is a scalar quantity that does not depend on x and y coordinates. Without loss of generality, we assume that the heterostructure is periodic in the z direction, and the wavevector of incident plane wave lies in the x–z plane. In the Cartesian coordinates, the electric and magnetic fields of this plane wave

#138472 - $15.00 USD Received 19 Nov 2010; revised 15 Dec 2010; accepted 15 Dec 2010; published 17 Dec 2010

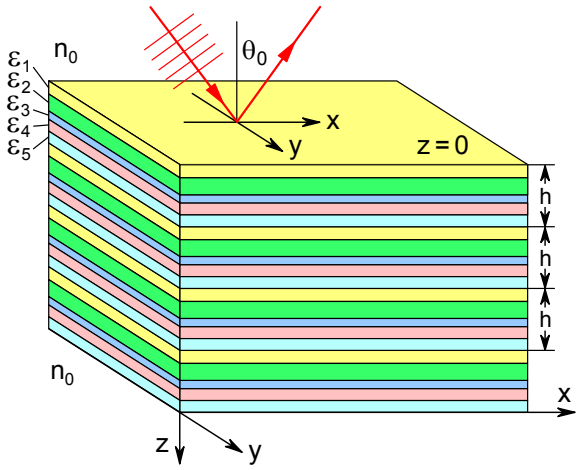

Fig. 1. Geometry of a periodic stratified heterostructure surrounded by a transparent media of refractive index n_0; h is the length of the unit cell. Plane electromagnetic wave obliquely incident in the x–z plane, at an angle ϑ_0 to the normal of the surface $z = 0$.

in the plane $z > 0$ can be written in the form

$$\mathbf{E}(x,z,t) = \begin{pmatrix} E_x \\ E_y \\ E_z \end{pmatrix} \exp[i(\beta x - \omega t)] + \text{c.c.}, \quad \mathbf{H}(x,z,t) = \begin{pmatrix} H_x \\ H_y \\ H_z \end{pmatrix} \exp[i(\beta x - \omega t)] + \text{c.c.},$$

where $\beta = n_0 k \sin\vartheta_0$ is the x component of the wavevector, $n_0 > 0$ is the refractive index of the medium surrounding the heterostructure, $k = \omega/c$, and c is the speed of light in vacuum.

In the adopted geometry, only four components of the vectors $\mathbf{E}$ and $\mathbf{H}$ are linearly independent. In the 4×4-matrix method, the problem of light propagation is formulated for the four tangential components that are continuous on the heterostructure interfaces, and form the elements of a four-dimensional vector defined as [34]

$$\psi(z) = \begin{pmatrix} E_x \\ H_y \\ E_y \\ -H_x \end{pmatrix}.$$

Using this vector, Maxwell's equations can be written in a compact form. It turns out that this vector satisfies a first-order differential equation of the form

$$\frac{\mathrm{d}\psi}{\mathrm{d}z} = ik\Delta(z)\psi, \tag{1}$$

where $\Delta(z)$ is a periodic 4×4 matrix characterizing optical properties of the heterostructure [34]. The other two components of the electromagnetic field inside any nonmagnetic, isotropic medium of permittivity ε can be found from the relations

$$E_z = -(\beta/k)(1/\varepsilon)H_y, \quad H_z = (\beta/k)E_y. \tag{2}$$

The specific form of the matrix $\Delta(z)$ depends on the heterostructure composition. We assume it to consists of m identical unit cells, each of which is made of n layers of thicknesses h_j

#138472 - $15.00 USD Received 19 Nov 2010; revised 15 Dec 2010; accepted 15 Dec 2010; published 17 Dec 2010

$(j = 1,2,\ldots,n)$ whose permittivities are constant within individual layers but change abruptly at the interfaces. Since Δ is independent of z inside each layer, Eq. (1) can be integrated to obtain the field within the jth layer in the form

$$\psi(z) = \exp(ik\Delta_j z)\psi(h_1 + h_2 + \ldots + h_{j-1}), \tag{3}$$

where $0 \le z \le h_j$ and Δ_j is the matrix inside the jth layer. In this notation, $\psi(h_1) = \exp(ik\Delta_1 h_1)\psi(0)$.

Since the layers are made of nonmagnetic and isotropic materials characterized by the permittivities ε_j $(j = 1,2,\ldots,n)$, the matrix exponential in this solution, $\mathscr{P}_j(z) \equiv \exp(ik\Delta_j z)$, called here the transfer matrix, has the following block-diagonal form [34]

$$\mathscr{P}_j(z) = \begin{pmatrix} \cos\phi_j & i\pi_j \sin\phi_j & 0 & 0 \\ (i/\pi_j)\sin\phi_j & \cos\phi_j & 0 & 0 \\ 0 & 0 & \cos\phi_j & i\sigma_j \sin\phi_j \\ 0 & 0 & (i/\sigma_j)\sin\phi_j & \cos\phi_j \end{pmatrix}, \tag{4}$$

where $\phi_j = k_{zj} z$, $\pi_j = k_{zj}/(\varepsilon_j k)$, $\sigma_j = k/k_{zj}$, and $k_{zj} = \left(\varepsilon_j k^2 - \beta^2\right)^{1/2}$. The two sub-blocks of this matrix describe propagation of π- and σ-polarized plane waves, respectively, also known as TM and TE modes [32]. Although these two waves are independent of each other, and the results for one of them can be obtained from the results of the other using the well known symmetry of Maxwell's equations, we consider both of them for comprehensiveness in what follows.

Using Eqs. (3) and (4), we can calculate the optical field at any position z within the first unit cell from the matrix relation

$$\psi(z) = \mathscr{G}_j(z)\psi(0), \tag{5}$$

where the translation matrix $\mathscr{G}_j$ is a product of multiple transfer matrices and is given by

$$\mathscr{G}_j(z) = \mathscr{P}_j(z)\mathscr{P}_{j-1}(h_{j-1}) \times \cdots \times \mathscr{P}_2(h_2)\mathscr{P}_1(h_1).$$

Extending this approach to the whole heterostructure, Eq. (5) solves the problem of light propagation through it. It should be recognized that in deriving Eq. (5) from Eq. (3), we used the fact that ψ is continuous at the interfaces between the layers.

2.2. Solution of the eigenvalue problem

Equation (5) itself is not very useful, since it does not explicitly contain information about the directions of the wavefront normal and energy flux inside the heterostructure. To find these directions, we need to analyze the evolution of the optical field within one heterostructure period. This evolution is governed by the unit-cell translation matrix $\mathscr{F}_h = \mathscr{G}_n(h_n)$, with the four eigenvalues [34]

$$q_\eta^{\pm} = K_\eta \pm \left(K_\eta^2 - 1\right)^{1/2}, \quad \eta = \pi \text{ or } \sigma. \tag{6}$$

The coefficient K_η is given by

$$K_\eta = \left(2^n \prod_{j=1}^{n} \eta_j\right)^{-1} \sum (-1)^r (\eta_1 \pm \eta_2)(\pm\eta_2 \pm \eta_3) \times \cdots \\ \cdots \times (\pm\eta_{n-1} \pm \eta_n)(\pm\eta_n + \eta_1)\cos(\varphi_1 \pm \varphi_2 \pm \ldots \pm \varphi_n),$$

#138472 - $15.00 USD Received 19 Nov 2010; revised 15 Dec 2010; accepted 15 Dec 2010; published 17 Dec 2010

where the sum is taken over 2^{n-1} possible sign combinations of the cosine argument, while ensuring that the signs in front of η_j ($=\pi_j$ or σ_j) and $\varphi_j = k_{zj}h_j$ ($j=2,3,\ldots,n$) are the same; r is the number of minuses in the expression $\varphi_1 \pm \varphi_2 \pm \ldots \pm \varphi_n$.

The four "normal" modes that correspond to the eigenvalues in Eq. (6) have the form

$$\psi_\pi^\pm = \begin{pmatrix} 1 \\ \Psi_\pi^\pm \\ 0 \\ 0 \end{pmatrix}, \qquad \psi_\sigma^\pm = \begin{pmatrix} 0 \\ 0 \\ 1 \\ \Psi_\sigma^\pm \end{pmatrix}, \tag{7}$$

where $\Psi_\pi^\pm = (q_\pi^\pm - F_{11})/F_{12}$, $\Psi_\sigma^\pm = (q_\sigma^\pm - F_{33})/F_{34}$, and F_{uv} are the elements of the matrix $\mathscr{F}_h$ given in Appendix A.

To proceed further, we need to specify which of the normal modes in Eq. (7) represent the waves moving in positive z direction. This is not as trivial a task as it might appear at first glance, for none of the signs in Eqs. (6) and (7) can be attributed to the wave traveling in the positive z direction, regardless of the material parameters (h_j and ε_j, $j=1,2,\ldots,n$). The reason for this is that the secular equation $\mathscr{F}_h\psi_\eta^\pm = q_\eta^\pm\psi_\eta^\pm$ does not determine the phase of the complex eigenvalues uniquely but only gives them up to a modulo factor of 2π, i.e.,

$$\arg q_\eta^\pm = \operatorname{Arg} q_\eta^\pm + 2\pi N, \quad N = 0, \pm 1, \pm 2, \ldots,$$

where $\operatorname{Arg} q_\eta^\pm \in (-\pi, \pi]$ is the principle value of the argument function. For the phase of the electromagnetic field to steadily grow, as the wave propagates through the heterostructure, we have to select different eigenvectors in different situations. It is possible to show (see Appendix B) that the η-polarized plane wave traveling in the positive z direction is described by the normal mode with

$$\operatorname{Re}\Psi_\eta^\pm > 0. \tag{8}$$

In what follows, we shall omit the superscripts $\pm$ for the elements Ψ_η satisfying this condition.

2.3. Refraction of wavefront and energy flux

The wavevectors of both the π-polarized and σ-polarized plane waves constantly vary during their propagation through a heterostructure slab. Inside the jth layer, the angle $\vartheta_{\mathbf{k},\pi,j}$ between the wavevector of the π-polarized plane wave and the z axis is characterized by the relation

$$\tan\vartheta_{\mathbf{k},\pi,j} = \frac{\beta}{\mathrm{d}(\operatorname{Arg} H_{yj})/\mathrm{dz}} = \frac{|H_{yj}|^2}{\operatorname{Re}(\varepsilon_j E_{xj} H_{yj}^*)}\frac{1}{k/\beta}, \quad (j=1,2,\ldots,n). \tag{9}$$

Here, according to Eqs. (5) and (7), $E_{xj} = G_{11}^{(j)} + G_{12}^{(j)}\Psi_\pi$ and $H_{yj} = G_{21}^{(j)} + G_{22}^{(j)}\Psi_\pi$, where $G_{uv}^{(j)}$ are the elements of the matrix $\mathscr{G}_j(z)$ given in Appendix A.

A similar expression holds for the direction of the wavevector of the σ-polarized wave:

$$\tan\vartheta_{\mathbf{k},\sigma,j} = \frac{\beta}{\mathrm{d}(\operatorname{Arg} E_{yj})/\mathrm{dz}} = -\frac{|E_{yj}|^2}{\operatorname{Re}(E_{yj} H_{xj}^*)}\frac{1}{k/\beta}, \tag{10}$$

where $E_{yj} = G_{33}^{(j)} + G_{34}^{(j)}\Psi_\sigma$ and $H_{xj} = -G_{43}^{(j)} - G_{44}^{(j)}\Psi_\sigma$.

Since E_z is discontinuous on heterostructure interfaces, the energy flux in the π-polarized plane wave refracts on each interface. In the jth layer, the tangent of the angle between the Poynting vector $\mathbf{S}$ and the z axis vary with wave propagation as

$$\tan\vartheta_{\mathbf{S},\pi,j} = -\frac{\operatorname{Re}(E_{zj}H_{yj}^*)}{\operatorname{Re}(E_{xj}H_{yj}^*)} = \frac{|H_{yj}|^2}{\operatorname{Re}(E_{xj}H_{yj}^*)}\frac{\operatorname{Re}(1/\varepsilon_j)}{k/\beta}. \tag{11}$$

#138472 - $15.00 USD Received 19 Nov 2010; revised 15 Dec 2010; accepted 15 Dec 2010; published 17 Dec 2010

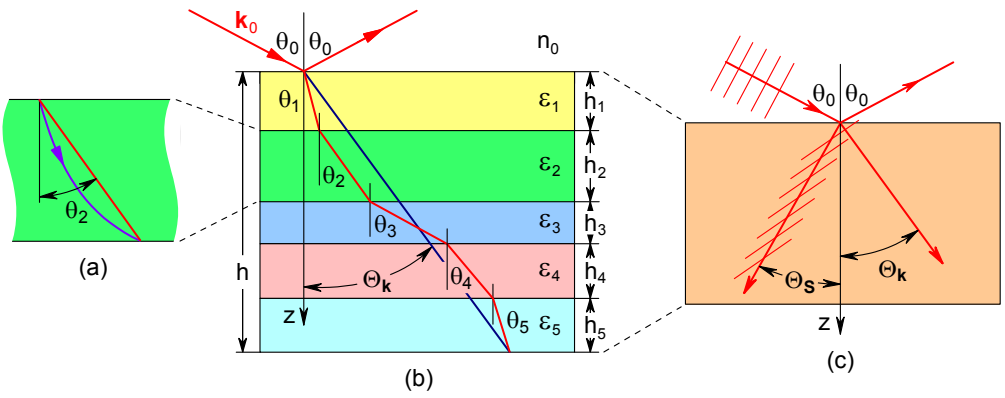

Fig. 2. Illustration of the averaging procedure in Eq. (13): (a) first, the direction of **k** is averaged within each layer; (b) resulting angles are then averaged over all layers in a unit cell. (c) Directions of energy flow and **k** for a π-polarized plane wave undergoing negative refraction inside a heterostructure slab with ultrathin layers.

In contrast, the energy flux in the σ-polarized plane wave does not refract on heterostructure interfaces. It is easy to see that its direction in the jth layer is characterized by the tangent

$$\tan\vartheta_{\mathbf{S},\sigma,j} = -\frac{\mathrm{Re}(E_{yj}H_{zj}^{*})}{\mathrm{Re}(E_{yj}H_{xj}^{*})} = \tan\vartheta_{\mathbf{k},\sigma,j}. \tag{12}$$

Hence, the energy flux in a σ-polarized plane wave propagating through a slab of stratified periodic heterostructure (composed of nonmagnetic layers) always refracts normally. This result is expected because the slab is isotropic with respect to the TE wave.

By looking at Eqs. (9)–(12), we immediately conclude that the four angles are equal only in the case of a single nonabsorbing slab. In all other cases, the first three angles are generally different. The form of Eq. (11) also suggests (see Appendix B) that $\mathrm{Re}\,\varepsilon_j < 0$ is required for at least one of the layers within a unit cell for a π-polarized plane wave to experience negative refraction. Of course, the layers with a negative real part of ε_j should be thick enough to substantially contribute to the effective permittivity of the slab, but thin enough to enable high transmissivity of the wave.

The effective direction $\Theta_{\mathbf{q},\eta}$ of the vector $\mathbf{q}$ ($=\mathbf{k}$ or $\mathbf{S}$) for the η-polarized plane wave can be found by averaging values of $\tan\vartheta_{\mathbf{q},\eta,j}$ over the thickness of each layer, followed by an average over the number of layers within a heterostructure period, i.e.,

$$\Theta_{\mathbf{q},\eta} = \tan^{-1}\left(\frac{1}{h}\sum_{j=1}^{n}\int_{0}^{h_j}\tan\vartheta_{\mathbf{q},\eta,j}\,\mathrm{d}z\right), \tag{13}$$

where $h = h_1 + h_2 + \ldots + h_n$. Figure 2 illustrates this definition. Physically, the angle $\Theta_{\mathbf{S},\eta}$ ($\eta = \pi, \sigma$) determines the parallel shift of the η-polarized optical beam caused by its single pass through the heterostructure slab.

2.4. Reflection and transmission coefficients

Once the eigenvectors of the unit-cell translation matrix and the normal modes of the heterostructure slab are known, we can calculate the reflection and transmission coefficients for the π- and σ-polarized plane waves. Remarkably, in the eigenvector formalism, these coefficients can be found analytically without resorting to the Chebyshev identity for the mth power of the unit-cell translation matrix [32, 33].

#138472 - $15.00 USD Received 19 Nov 2010; revised 15 Dec 2010; accepted 15 Dec 2010; published 17 Dec 2010

The mth power of the translation matrix $\mathscr{F}_h$ relates the field at the output heterostructure surface, $\psi_\eta^\pm(mh)$, to that at the input surface, $\psi_\eta^\pm$. This power is eliminated by employing the eigenvalue equation $(\mathscr{F}_h)^m\psi_\eta^\pm = \left(q_\eta^\pm\right)^m\psi_\eta^\pm$ $(\eta=\pi,\sigma)$. The electromagnetic boundary conditions at $z=0$ and $z=mh$ require that the input, transmitted, and reflected fields, ψ_i, ψ_t, and ψ_r, satisfy the equations

$$\psi_i+\psi_r = A_\pi^+\psi_\pi^+ + A_\pi^-\psi_\pi^- + A_\sigma^+\psi_\sigma^+ + A_\sigma^-\psi_\sigma^-, \tag{14a}$$

$$\psi_t = A_\pi^+Q_\pi^+\psi_\pi^+ + A_\pi^-Q_\pi^-\psi_\pi^- + A_\sigma^+Q_\sigma^+\psi_\sigma^+ + A_\sigma^-Q_\sigma^-\psi_\sigma^-, \tag{14b}$$

where $Q_\eta^\pm = \left(q_\eta^\pm\right)^m$ and $A_\eta^\pm$ $(\eta=\pi,\sigma)$ are the normalized complex-valued amplitudes of the normal modes inside the slab.

The input, transmitted, and reflected fields are described by the four-dimensional vectors

$$\psi_i = \begin{pmatrix} 1 \\ r_\pi \\ 1 \\ r_\sigma \end{pmatrix}, \quad \psi_r = \begin{pmatrix} R_\pi \\ -r_\pi R_\pi \\ R_\sigma \\ -r_\sigma R_\sigma \end{pmatrix}, \text{ and } \psi_t = \begin{pmatrix} T_\pi \\ r_\pi T_\pi \\ T_\sigma \\ r_\sigma T_\sigma \end{pmatrix},$$

where $r_\pi = n_0\sec\vartheta_0$ and $r_\sigma = n_0\cos\vartheta_0$. The system of eight linear equations (14) for the unknowns $A_\eta^\pm$, R_η, and T_η $(\eta=\pi,\sigma)$ is readily solved to obtain

$$A_\eta^\pm = \mp 2r_\eta Q_\eta^\mp(\Psi_\eta^\mp - r_\eta)/D_\eta, \tag{15a}$$

$$R_\eta = (Q_\eta^- - Q_\eta^+)(\Psi_\eta^+ - r_\eta)(\Psi_\eta^- - r_\eta)/D_\eta, \tag{15b}$$

$$T_\eta = 2r_\eta Q_\eta^+Q_\eta^-(\Psi_\eta^+ - \Psi_\eta^-)/D_\eta, \tag{15c}$$

where $D_\eta = Q_\eta^+(\Psi_\eta^+ - r_\eta)(\Psi_\eta^- + r_\eta) - Q_\eta^-(\Psi_\eta^+ + r_\eta)(\Psi_\eta^- - r_\eta)$.

We can see that, in the limit $h\to 0$, the matrix $\mathscr{F}_h$ becomes a unit matrix. Since $Q_\eta^\pm \to 1$ in this limit, Eqs. (15b) and (15c) reduce to $R_\eta = 0$ and $T_\eta = 1$. It can also be verified that $|R_\eta|^2 + |T_\eta|^2 = 1$ in the absence of optical losses. When absorption inside layers is included through their complex permittivity, total losses can be characterized by the coefficient $D_\eta = 1 - |R_\eta|^2 - |T_\eta|^2$.

3. Negative refraction in the limit of ultrathin layers

The problem of negative refraction in stratified media is particularly simple for ultrathin layers, i.e., when the heterostructure period is much shorter than the wavelength of light $(kh \ll 1)$. We treat this situation separately, to illustrate the application of the formalism developed in Section 2.

When $\phi_j \ll 1$ for all layers $(j=1,2,\ldots,n)$, the trigonometric functions in Eq. (4) can be approximated by the first terms of their Taylor series. As a result, the unit-cell translation matrix takes the simple form

$$\mathscr{F}_h = \begin{pmatrix} 1 & ik_\perp^2 h/(\varepsilon_\perp k) & 0 & 0 \\ i\varepsilon_\parallel kh & 1 & 0 & 0 \\ 0 & 0 & 1 & ikh \\ 0 & 0 & ik_\parallel^2 h/k & 1 \end{pmatrix}, \tag{16}$$

where $k_\perp = \left(\varepsilon_\perp k^2 - \beta^2\right)^{1/2}$, $k_\parallel = \left(\varepsilon_\parallel k^2 - \beta^2\right)^{1/2}$, and the components of the effective permittivity tensor are given by

$$\varepsilon_{xx} = \varepsilon_{yy} \equiv \varepsilon_\parallel = \frac{1}{h}\sum_{j=1}^n h_j\varepsilon_j, \quad \varepsilon_{zz} \equiv \varepsilon_\perp = \left(\frac{1}{h}\sum_{j=1}^n \frac{h_j}{\varepsilon_j}\right)^{-1}.$$

#138472 - $15.00 USD Received 19 Nov 2010; revised 15 Dec 2010; accepted 15 Dec 2010; published 17 Dec 2010

The eigenvalues and eigenvectors of the translation matrix (16) are easy to find. The eigenvalues are given by

$$q_\pi^\pm = 1 \pm ik_\perp h(\varepsilon_\parallel/\varepsilon_\perp)^{1/2}, \quad q_\sigma^\pm = 1 \pm ik_\parallel h.$$

The normal modes are given by Eq. (7) with the elements

$$\Psi_\pi^\pm = \pm(k/k_\perp)(\varepsilon_\parallel\varepsilon_\perp)^{1/2}, \quad \Psi_\sigma^\pm = \pm k_\parallel/k.$$

Using these results in Eqs. (9)–(13), the four angles are found to be

$$\tan\Theta_{\mathbf{k},\pi} \approx \pm\frac{\beta}{\mathrm{Re}\left[k_\perp(\varepsilon_\parallel/\varepsilon_\perp)^{1/2}\right]}, \quad \tan\Theta_{\mathbf{S},\pi} \approx \pm\frac{\beta|\varepsilon_\parallel|\,\mathrm{Re}(1/\varepsilon_\perp)}{\mathrm{Re}\left[k_\perp(\varepsilon_\parallel^*/\varepsilon_\perp)^{1/2}\right]}, \tag{17}$$

$$\Theta_{\mathbf{k},\sigma} = \Theta_{\mathbf{S},\sigma} \approx \pm\tan^{-1}\left(\frac{\beta}{\mathrm{Re}\,k_\parallel}\right), \tag{18}$$

where the plus or minus sign should be taken to comply with the requirement in Eq. (8). In deriving Eqs. (17) and (18), we neglected the variation of the optical field within the unit cell.

Equation (17) shows that, in the limit of ultrathin layers, the effect of negative refraction occurs for frequencies that satisfy the condition $\mathrm{Re}\,\varepsilon_\perp(\omega) < 0$. At certain frequency ω_0, the real part of the transverse permittivity may vanish, leading to $\Theta_{\mathbf{S},\pi} = 0$ regardless of the incident angle ϑ_0. That means that any TM wave incident obliquely on the heterostructure slab propagates in the z direction. This effect can be used to collect light coming from all spatial directions within a narrow spectral band around ω_0.

4. A periodic heterostructure composed of two semiconductors

We now consider in more detail a periodic heterostructure with two layers in its unit cell. The expressions for the elements of the translation matrix $\mathscr{G}_j(z)$ that correspond to this situation are given in Appendix B. For numerical examples, we focus on the case in which two layers in each unit cell are made of p-doped InGaAs (p-InGaAs) and intrinsic AlInAs semiconductors characterized by the permittivities [19]

$$\varepsilon_1(\omega) = 12.15 \times \left(1 - \frac{\omega_p^2}{\omega(\omega + i\delta)}\right)$$

and $\varepsilon_2 = 10.23$, respectively, where ω_p is the plasma frequency at the free-carrier density of 7.5×10^{18} cm^{-3}, and $\delta = 10^{13}$ rad/s. The effect of negative refraction may then occur at frequencies below $\omega_0 = (\omega_p^2 - \delta^2)^{1/2}$, which approximately corresponds to the wavelength of 8.8 μm. We also assume that the heterostructure slab is surrounded by air ($n_0 = 1$). It should be stressed that our analysis is not limited to only heterostructures made with semiconductor materials, and can be used even for heterostructures in which some or all layers are made of metals.

In Figs. 3(a) and 3(b), we plot the effective refraction angles for the energy flux and wavevector for a π-polarized beam incident at an angle of $\pi/3$ on the heterostructure surface. The blue and red curves correspond to 2- and 0.2-μm-thick layers, respectively; open circles show the approximate solution calculated with Eq. (17) valid only for thin layers. In the case of thin layers, the beam refracts at negative angles within the wavelength range from 8.8 to 11.9 μm marked by the red shaded band. As discussed earlier, this band coincides precisely with the range where $\mathrm{Re}\,\varepsilon_\perp < 0$ [see the wine-color curve in Fig. 3(a)]. In the heterostructure with thick layers, the phenomenon of negative refraction occurs within a much narrower band (shaded in blue) with a larger absolute value of the maximum refraction angle.

#138472 - $15.00 USD Received 19 Nov 2010; revised 15 Dec 2010; accepted 15 Dec 2010; published 17 Dec 2010

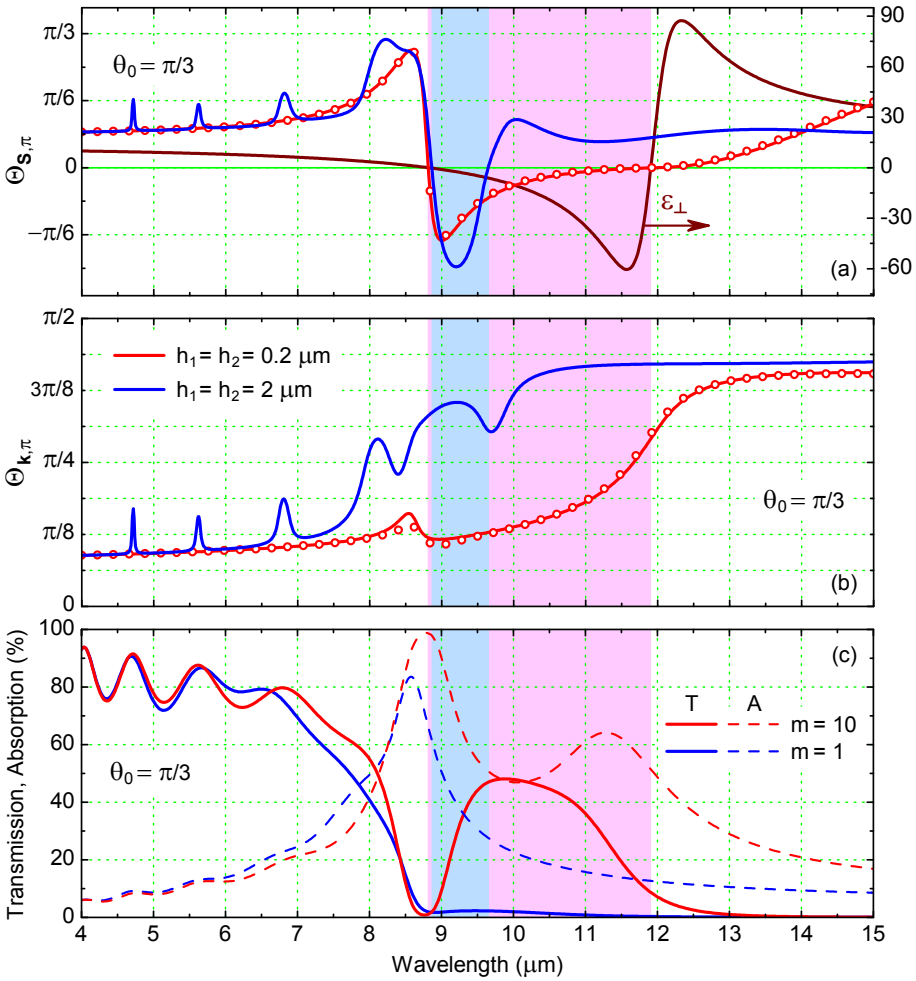

Fig. 3. Effective refraction angles of (a) energy flux and (b) wavevector for a π-polarized plane wave incident at an angle $\vartheta_0 = \pi/3$ on a heterostructure made with 0.2- and 2-μm-thick layers; the shaded bands show the regions of negative refraction in the two cases; open circles correspond to the approximate solution in Eq. (17). (c) Transmission (T) and absorption (A) spectra for 4-μm-thick slabs made of thick (blue) and thin (red) layers.

It is important to compare the transmissivity of heterostructure slabs with different layer thicknesses. For such comparison to be fair, the total thicknesses of the slabs should be equal. As an example, Fig. 3(c) shows the transmission and absorption spectra for two 4-μm-thick slabs; one slab contains twenty 0.2-μm-thick layers (red curves), while the second slab is made of only two 2-μm-thick layers (blue curves). One can see that the transmissivity of thin layers is considerably higher than that of thick layers within the negative refraction band. This difference is not due to stronger optical absorption by the second slab. In fact, as the dashed curves show, absorption is much larger within the negative refraction band for the structure with thin layers. Therefore, it is the higher reflection that drastically reduces the transmissivity of the second slab.

The effective angles $\Theta_{\mathbf{S},\sigma} = \Theta_{\mathbf{k},\sigma}$ and the transmission spectra for the σ-polarized beam are shown in Fig. 4 under the conditions identical to those used for Fig. 3. A comparison of these

#138472 - $15.00 USD Received 19 Nov 2010; revised 15 Dec 2010; accepted 15 Dec 2010; published 17 Dec 2010

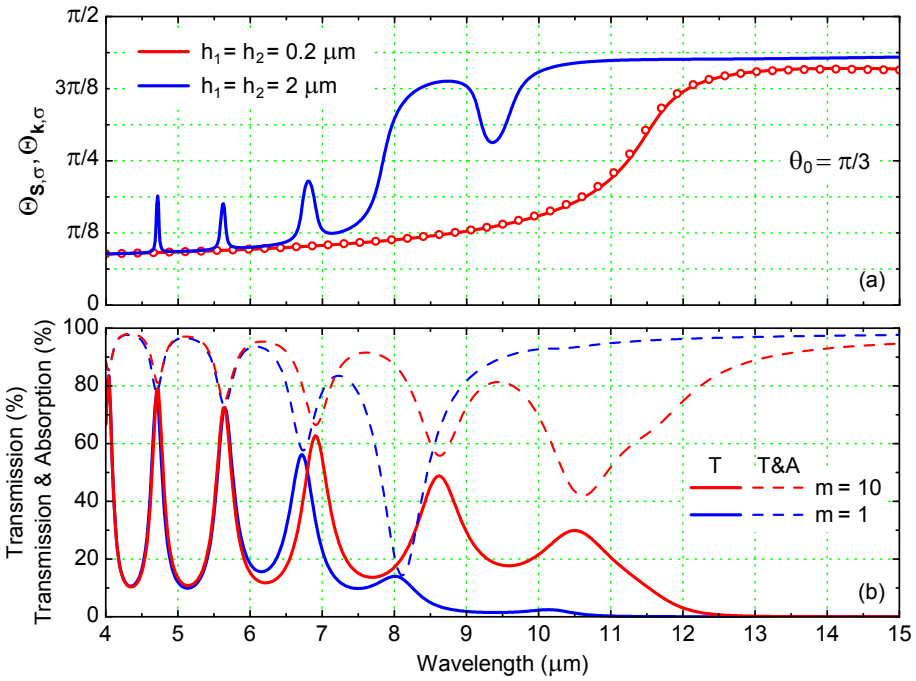

Fig. 4. (a) Effective refraction angles of energy flux and wavevector for a σ-polarized plane wave incident at an angle $\vartheta_0 = \pi/3$ on a heterostructure made with 0.2- and 2-μm-thick layers; circles correspond to the approximate solution in Eq. (18). (b) Transmission (T) and transmission plus absorption (T&A) spectra for 4-μm-thick slabs made of thick (blue) and thin (red) layers.

two figures shows that the wavefronts of π- and σ-polarized beams refract similarly, regardless of the layers' thicknesses. It is also interesting to note that, within the band of negative refraction for π polarization, the transmissivity of thin layers with respect to the σ-polarized beam is much higher than the transmissivity of thick layers. The reason behind this fact, however, differs from the one given above for π polarization. As indicated in Fig. 4(b), the reflectivity from thin layers in this case is higher compared to that from thin layers, and the poor transmissivity predominantly results from stronger absorption.

Figure 5 shows the angular dependence of the refraction angles $\Theta_{\mathbf{S},\pi}$ and $\Theta_{\mathbf{k},\pi}$, as well as the transmission, reflection, and absorption coefficients for the two 4-μm-thick slabs with twenty thin and two thick layers. These results support our previous conclusions and reveal a further difference in the properties of the two slabs. According to Eq. (17), when the wavelength is close to the band edge of negative refraction, the energy propagates through the slab made of thin layers perpendicular to its surface, whatever the incident angle is. This effect is illustrated in Fig. 5(a) for $\lambda = 8.8137$ μm. The picture is completely different when the layers are thick. In that case, normal and negative refractions switch at certain incident angles $\pm\vartheta_c$, as shown in Fig. 5(b) for $\lambda = 8.84$ μm. If the incident angle lies in the range $-\vartheta_c < \vartheta_0 < \vartheta_c$, the π-polarized beam exhibits negative refraction; otherwise, it refracts normally. In addition to small transmissivity [see Fig. 5(d)], the absolute values of $\Theta_{\mathbf{S},\pi}$ for $|\vartheta_0| < \vartheta_c$ are relatively small; further investigation is required to make this effect suitable for practical applications.

We should also point out that our analysis can be readily generalized to the case of layers that possess magnetic properties. In this situation, $H_{zj} = (\beta/k)(1/\mu_j)E_{yj}$, where μ_j $(j = 1, 2, \ldots, n)$

#138472 - $15.00 USD Received 19 Nov 2010; revised 15 Dec 2010; accepted 15 Dec 2010; published 17 Dec 2010

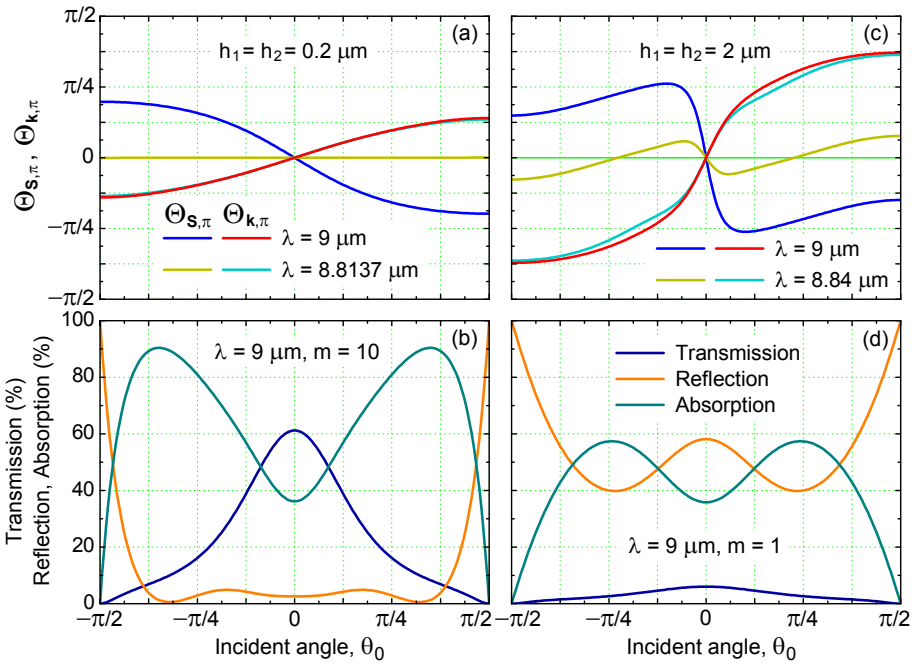

Fig. 5. Effective refraction angles of energy flux and wavevector [(a), (c)] and transmission, reflection, and absorption coefficients [(b), (d)] for a π-polarized beam incident at different angles on heterostructures made of thin [(a), (b)] and thick [(c), (d)] layers.

are the permeabilities, and one should use the functions $\sigma_j = \mu_j k/k_{zj}$ and $k_{zj} = \left(\varepsilon_j \mu_j k^2 - \beta^2\right)^{1/2}$ in Eq. (4). However, the form of Eqs. (6)–(11), (13)–(15), and (17) does not change in the magnetic case.

5. Conclusions

Using the 4×4-matrix formalism of Berreman [34], we have developed a simple theory of negative refraction in periodic stratified heterostructures composed of homogeneous, isotropic, nonmagnetic layers. We derived analytic expressions for the normal modes of heterostructure slabs with an arbitrary number of layers in a unit cell. We introduced suitable definitions for the average refraction angles, associated with the energy flow and the wave vector, for the TE- and TM-polarized plane waves falling obliquely on the heterostructure slab. We also derived general expressions for the reflectivity and transmissivity of such plane waves, and applied them to study negative refraction by a slab of ultrathin layers for which simple approximate formulae for the average refraction angles can be obtained. A numerical investigation of a heterostructure with two semiconductor layers per unit cell revealed that ultrathin layers are preferable to thick layers for optical applications, as they facilitate higher transmissivity within the frequency band of negative refraction; this feature does not appear to have been noted in previous work. Our results are valid for heterostructures containing metallic layers, and provide a well-needed theoretical treatment for stratified periodic metamaterials.

#138472 - $15.00 USD Received 19 Nov 2010; revised 15 Dec 2010; accepted 15 Dec 2010; published 17 Dec 2010

Appendix A

The matrix $\mathscr{G}_j(z)$ in Eq. (5) has the same block diagonal form as the matrix $\mathscr{P}_j(z)$ in Eq. (4). Its four elements appearing in the top block can be written as follows:

$$G_{11}^{(j)}(z) = \left(2^{j-1}\prod_{p=1}^{j-1}\pi_p\right)^{-1}\sum(-1)^s(\pi_1\pm\pi_2)(\pm\pi_2\pm\pi_3)\times\cdots$$
$$\cdots\times(\pm\pi_{j-1}\pm\pi_j)\cos(\varphi_1\pm\varphi_2\pm\ldots\pm\varphi_{j-1}\pm\phi_j), \quad (19a)$$

$$G_{12}^{(j)}(z) = i\left(2^{j-1}\prod_{p=2}^{j-1}\pi_p\right)^{-1}\sum(-1)^s(\pi_1\pm\pi_2)(\pm\pi_2\pm\pi_3)\times\cdots$$
$$\cdots\times(\pm\pi_{j-1}\pm\pi_j)\sin(\varphi_1\pm\varphi_2\pm\ldots\pm\varphi_{j-1}\pm\phi_j), \quad (19b)$$

$$G_{21}^{(j)}(z) = i\left(2^{j-1}\prod_{p=1}^{j}\pi_p\right)^{-1}\sum(-1)^r(\pi_1\pm\pi_2)(\pm\pi_2\pm\pi_3)\times\cdots$$
$$\cdots\times(\pm\pi_{j-1}\pm\pi_j)\sin(\varphi_1\pm\varphi_2\pm\ldots\pm\varphi_{j-1}\pm\phi_j), \quad (19c)$$

and

$$G_{22}^{(j)}(z) = \left(1+G_{21}^{(j)}G_{12}^{(j)}\right)/G_{11}^{(j)},$$

where the sums are taken over 2^{j-1} possible sign combinations in the arguments of the sine and cosine functions, while ensuring that the signs in front of the parameters π_p and φ_p ($p=2,3,\ldots,j$) are the same; s is the number of minuses in the expression $\varphi_1\pm\varphi_2\pm\ldots\pm\varphi_{j-1}$ and r is the number of minuses in the expression $\varphi_1\pm\varphi_2\pm\ldots\pm\varphi_{j-1}\pm\phi_j$.

The elements $G_{33}^{(j)}$, $G_{34}^{(j)}$, $G_{43}^{(j)}$, and $G_{44}^{(j)}$ associated with the second block are obtained, respectively, from $G_{11}^{(j)}$, $G_{12}^{(j)}$, $G_{21}^{(j)}$, and $G_{22}^{(j)}$ by the replacement $\pi_p\to\sigma_p$ ($p=1,2,\ldots,j$). The elements of the matrix $\mathscr{F}_h$ are obtained from those of the matrix $\mathscr{G}_j(z)$ after noting the definition $F_{uv}=G_{uv}^{(n)}(h_n)$.

When the unit cell of a periodic heterostructure has only two layers, one can use Eq. (19) to perform the sum explicitly and obtain the following analytic expressions:

$$G_{11}^{(2)} = \frac{1}{2\pi_1}\left[(\pi_1+\pi_2)\cos(\varphi_1+\phi_2)+(\pi_1-\pi_2)\cos(\varphi_1-\phi_2)\right],$$
$$G_{12}^{(2)} = \frac{i}{2}\left[(\pi_1+\pi_2)\sin(\varphi_1+\phi_2)+(\pi_1-\pi_2)\sin(\varphi_1-\phi_2)\right],$$
$$G_{21}^{(2)} = \frac{i}{2\pi_1\pi_2}\left[(\pi_1+\pi_2)\sin(\varphi_1+\phi_2)-(\pi_1-\pi_2)\sin(\varphi_1-\phi_2)\right].$$

The coefficient K_π appearing in Eq. (6) in this case is reduced to

$$K_\pi = \frac{1}{4\pi_1\pi_2}\left[(\pi_1+\pi_2)^2\cos(\varphi_1+\varphi_2)-(\pi_1-\pi_2)^2\cos(\varphi_1-\varphi_2)\right].$$

Appendix B

Let us first prove that Eq. (8) holds for the π-polarized plane wave moving in the $+z$ direction. The field of this wave in the jth layer satisfies Eq. (1). This equation can be written in the form

$$\frac{\mathrm{d}}{\mathrm{d}z}\begin{pmatrix}E_{xj}\\H_{yj}\end{pmatrix} = ik\begin{pmatrix}0 & \varpi_j\\ \varepsilon_j & 0\end{pmatrix}\begin{pmatrix}E_{xj}\\H_{yj}\end{pmatrix}, \quad (20)$$

#138472 - $15.00 USD Received 19 Nov 2010; revised 15 Dec 2010; accepted 15 Dec 2010; published 17 Dec 2010

where $\varpi_j = 1 - \beta^2/(k^2\varepsilon_j)$ and ε_j are the elements of the matrix $\Delta(z)$ [34]. Since the phase of the electric field must build up during its propagation, we can write

$$\frac{\mathrm{d}(\mathrm{Arg}\, E_{xj})}{\mathrm{d}z} = \frac{\mathrm{d}}{\mathrm{d}z}\left[\tan^{-1}\left(\frac{\mathrm{Im}\, E_{xj}}{\mathrm{Re}\, E_{xj}}\right)\right] > 0.$$

Using Eq. (20), we obtain the condition

$$\mathrm{Re}\left(\varpi_j E_{xj}^* H_{yj}\right) > 0. \tag{21}$$

A similar condition for the magnetic field, $\mathrm{d}(\mathrm{Arg}\, H_{yj})/\mathrm{d}z > 0$, results in

$$\mathrm{Re}\left(\varepsilon_j E_{xj} H_{yj}^*\right) > 0. \tag{22}$$

Equations (21) and (22) show that

$$\mathrm{Re}\left(E_{xj}^* H_{yj}\right) > 0,$$

which proves our above statement that negative refraction requires $\mathrm{Re}\,\varepsilon_j < 0$ for at least one heterostructure layer. The last inequality holds for any z within the jth layer. Specifically, at the point $z = 0$ inside the first layer, where the matrix $\mathscr{G}_1(0)$ is unitary, it reduces to the desired result $\mathrm{Re}\,\Psi_\pi > 0$.

Equation (8) can be proved for the σ-polarized plane wave in a similar fashion. In this case, we have

$$\frac{\mathrm{d}}{\mathrm{d}z}\begin{pmatrix} E_{yj} \\ -H_{xj} \end{pmatrix} = ik\begin{pmatrix} 0 & 1 \\ \varepsilon_j\varpi_j & 0 \end{pmatrix}\begin{pmatrix} E_{yj} \\ -H_{xj} \end{pmatrix}.$$

The inequality $\mathrm{Re}\,\Psi_\sigma > 0$ readily follows from the analog of Eq. (21)

$$\mathrm{Re}\left(E_{yj} H_{xj}^*\right) < 0.$$

Acknowledgments

The work of I. D. Rukhlenko, M. Premaratne, and G. P. Agrawal was sponsored by the Australian Research Council (ARC) through its Discovery Grant scheme under grants DP0877232 and DP110100713. The work of G. P. Agrawal was also supported by the NSF Award ECCS-0801772.

#138472 - $15.00 USD Received 19 Nov 2010; revised 15 Dec 2010; accepted 15 Dec 2010; published 17 Dec 2010